

# Heat Transfer and Thin Film Flow Analysis of EG-ZnO Nanofluids with Different Shape Factors over an Unsteady Radially Stretching Sheet

Abdul Wahid<sup>a1</sup>, Azeem Shahzad<sup>a</sup>

abwahid4065@gmail.com, azeem.shahzad@uettaxila.edu.pk

Department of Mathematical Sciences, University of Engineering and Technology Taxila 47080, Pakistan.

---

## ABSTRACT

This study explores the flow and heat transfer characteristics of a nanofluid layer near an unsteady radially stretched sheet. The complex nonlinear partial differential equations governing energy and motion are transformed into ordinary differential equations using similarity transformations. The simplified equations are solved numerically, enabling the calculation of temperature and velocity profiles. This work is unique in its focus on thin film flow over a radially stretched sheet. Various factors, such as the Eckert number, Prandtl number, and unsteadiness parameter, are analyzed in relation to their effects on flow and heat transfer. The results indicate that an increase in the unsteadiness parameter leads to a reduction in film thickness.

**Keywords:** Nano fluid, Thin Film, Radially Stretching, MHD,

---

Date of Submission: 07-11-2024

Date of acceptance: 19-11-2024

---

## I. Introduction

Nanofluids are a particular kind of liquid that have tiny particles called nanoparticles in it. The term "nanofluids" refers to the fact that these nanoparticles are usually between one and one hundred nanometers in size. Metals, metal oxides, or compounds based on carbon can all be used to create the nanoparticles. These nanoparticles produce a new kind of fluid with improved qualities when they are added to a base fluid, like water or oil. The enhanced heat transmission capacity of nanofluids is one of its key benefits. The fluid's ability to transmit heat more effectively is improved by the presence of nanoparticles, which increases its thermal conductivity. These nanoparticles produce a new kind of fluid with improved qualities when they are added to a base fluid, like water or oil. The enhanced heat transmission capacity of nanofluids is one of its key benefits [1, 2]. Heat carriers are an important component of many industrial processes, and this function is served by fluids. Basically, the behavior of fluids in thermal systems, such as car radiators to nuclear reactors, dictate the performance of such systems. Thermal systems are all about heat and so, the efficiency of the system can be boosted through the optimization of heat transfer. Heat transfer enhancement may lead to smaller thermal equipment and hence more energy and space efficiency and less cost. Active and passive techniques, which are used for enhancing heat transfer in many applications, have been reported. "Active" refers to the situation where some form of force from outside is applied to enhance heat transfer in a particular thermal device through for instance application of a magnetic field or vibration on the surface. On the other hand, "passive" refers to technologies where there is no external force, such as the fins and turbulators for enhancing the heat transfer rate. Employing nanofluids in lieu of conventional liquids in thermal systems is another passive approach to heat transfer enhancement. The main constraint in heat transfer applications has been the poor thermal conductivity of standard working fluids like water, EG, and EO. Recently, nanofluids that possess higher thermal conductivity than these base liquids have been developed for enhancing the heat transfer in several applications [3-8]. It should be born in mind that convective heat transfer in nanofluids depends on the flow pattern, volume fraction of the nanofluid and the geometrical arrangement of particles [9]. To begin with, the nanofluid has been captured in one's diction by Choi[10] who explained the fluid was resulted from nanoparticles distributed in a fluid. Subsequently, Masuda et al. [11] extended this notion of this analysis and studies in due course, an enormous amount of research was actively practiced in this line of research. In the recent years, many industries have introduced nanofluids into their systems and its analysis and numerical methods have motivated researchers in several disciplines of engineering [12-15]. For example, Sheikholeslami et al [16] have reviewed the effective valorization of nanofluids in between two rotating disks. In this process, they showed that during injection and suction process, the rate of heat transfer can be optimized by increasing the volume fraction of nanoparticles. In

In addition, Hatami and Ganji [17] employed the analytical Least square method (LSM) to analyze the effect of Cu-water nanofluid flow on the MCHS cooling system. The analytical method that they proposed for the solution of heat transfer problems was later applied also to other problems via the simplicity and high accuracy [18-20]. Therefore, Hatami and Ganji [20] investigated the effect of variable magnetic field on the flow characteristics of a nanofluid between two disks.

The aim of this paper is to provide a brief review of thin film flow and heat transfer over an unsteady radially stretching sheet. Given the wide range of applications for ethylene glycol, particularly in heat transfer systems, ethylene glycol nanoparticles were considered for this study. Consequently, the objective of this research is to address the specific effects on thin film flow and heat transfer involving ethylene glycol nanoparticles on a stretching sheet. A comparative study will be presented to analyze the trends in velocity, film thickness, temperature, Nusselt number, and skin friction with respect to different nanoparticle shapes. The conclusion will discuss how the shape of the particles influences these properties. The findings of this study could contribute to the development of new and improved heat transfer systems.

**Mathematical Formulation**

The present study deals with the unsteady, two-dimensional time MHD boundary layer flow analysis of a nanofluid on a thin liquid film considering the constant radial stretching sheet which contains the plain at  $z = 0$  the sheet starts moving as per the plan and moves radially with the velocity  $U(r, t) = \left(\frac{br}{(1-\alpha t)}\right)$ , where  $b$  is a constant with the dimensions of  $\text{time}^{-1}$  while  $\alpha$  is another constant having the same dimensions as  $b$ . Under this condition, the surface temperature of a stretched sheet is given  $T_{s(r,t)} = T_0 - T_{ref} \left[\frac{br^2}{2\nu}\right] (1 - \alpha t)^{-\frac{3}{2}}$ , the variables used here have the following meanings  $T_s$  is slit temperature and  $T_{ref}$  is a constant reference temperature such that  $0 \leq T_{ref} \leq T_0$ ,  $h$  is thickness of the liquid film. Some of the parameters may have more details in them as following in nomenclature.

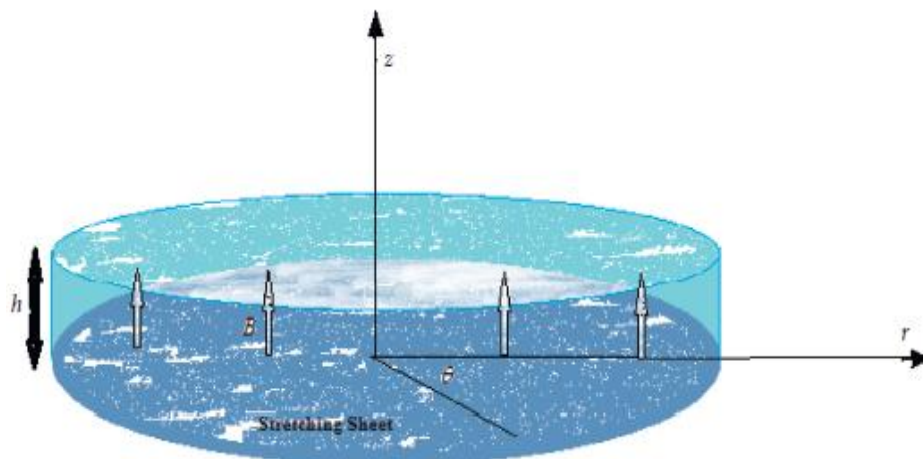


Figure 1: Physical interpretation

The real-world phenomenal model showed mathematically is illustrated in Fig 1 by cylindrical polar co-ordinates  $(r, \theta, z)$ . Due to the axisymmetric of the flow, all physically relevant quantities do not depend on  $\theta$ . It specified that the velocity profile is  $v = [u(r, z), 0, w(r, z)]$  where  $w$  and  $u$  are velocities in radial and  $z$  direction respectively. Accordingly, from the basic governing equation for momentum, energy and mass, the following as :

$$\frac{\partial u}{\partial r} + \frac{u}{r} + \frac{\partial w}{\partial z} = 0, \tag{1}$$

$$\left(\frac{\partial u}{\partial t} + u \frac{\partial u}{\partial r} + w \frac{\partial u}{\partial z}\right) = \gamma_{nf} \left(\frac{\partial^2 u}{\partial z^2}\right), \tag{2}$$

$$\frac{\partial T}{\partial t} + u \frac{\partial T}{\partial r} + w \frac{\partial T}{\partial z} = \frac{\partial^2 T}{\partial z^2} \frac{K_{nf}}{(\rho c_p)_{nf}} + \frac{\mu_{nf}}{(\rho c_p)_{nf}} \left(\frac{\partial u}{\partial z}\right)^2, \tag{3}$$

Here  $T$  shows the temperature of the nanofluid,  $\nu$  denotes the kinematic viscosity, and electrical conductivity  $\sigma$ , fluid density  $\rho$ ,  $\alpha = \left(\frac{\kappa}{\rho C_p}\right)$  stands for the thermal diffusivity of the fluid,  $C_p$  is the specific heat at stable pressure, and  $\kappa$  represents the thermal conductivity. Related BCs are specified as follows.

$$u = U, w = 0, T = T_s, z = 0, \tag{4}$$

$$\frac{\partial u}{\partial z} + \frac{\partial T}{\partial z} = 0, u = \frac{dh}{dt}, z = h. \tag{5}$$

Continuing with the study, we made the following similarity transformation.

$$\psi = -r^2 U Re^{-\frac{1}{2}} f(\eta), \eta = \frac{z}{r} Re^{\frac{1}{2}}, \theta(\eta) = \frac{T_o - T(r,z)}{T_{ref}(br^2/(2\nu(1-\alpha t)^{\frac{3}{2}}))}, \tag{6}$$

In this equation  $\psi(r, z)$  is Stoke stream function,  $\eta$  is independent variable with  $u = -\frac{1}{r} \frac{\partial \psi}{\partial z}$ ,  $w = \frac{1}{r} \frac{\partial \psi}{\partial r}$ , and  $Re = \frac{rU}{\nu}$  is local Reynolds parameter. Velocity component is defined below:

$$u = U f'(\eta), w = -2U Re^{-\frac{1}{2}} f(\eta). \tag{7}$$

The set of similarity transformations discussed complied with this law of conservation of mass as depicted in the equation (1). Therefore, the analytical problem set out by the equations (2)-(5) is changed with a set of ordinary differential equations as follows,

$$Sf' + Sf''\eta - 2f''f + f'^2 = f''' \epsilon_1, \tag{8}$$

$$\theta'' \epsilon_2 - Pr \left( \frac{S}{2} (3\theta + \eta\theta') + 2\theta f' - 2f\theta' \right) = 0. \tag{9}$$

$$\epsilon_1 = \frac{1 + iA_1 \phi + A_2 \phi^2}{\left( 1 - \phi + \phi \left( \frac{\rho_s}{\rho_f} \right) \right)}, \quad \epsilon_2 = \frac{\frac{k_{nf}}{k_f}}{\left( 1 - \phi + \phi \left( \frac{(\rho C_p)_s}{(\rho C_p)_f} \right) \right)},$$

where BC's are

$$f'(0) = 1, f(0) = 0, \quad \theta(0) = 1, \tag{10}$$

$$f''(\beta) = 0, \theta'(\beta) = 0, f(\beta) = \frac{S\beta}{4}. \tag{11}$$

Here,  $S = (\alpha/b)$  is the dimensionless measure of the unsteadiness number,  $M = (\sigma B^2/\rho b)$  is the magnetic parameter,  $Pr = (\nu/\alpha)$  is the Prandtl number,  $Ec = (U^2/C_p \nabla T)$  is the Eckert parameter while prime demonstrate derivate with respect to  $\eta$ . (Unknown Constant)  $\beta$  is dimensionless thickness of the film may be inclined as,  $\beta = \left( \frac{b}{\nu(1-\alpha t)^{\frac{1}{2}}} \right) h$ . Differentiate  $h$  with regard to  $t$  yields the level at which film thickness varies. Thus, the reduced differential of the velocity is given by  $\left( \frac{dh}{dt} \right) = (-\alpha\beta/2)(\nu/b(1-\alpha t)^{(1/2)})$ . Thus, the Nusselt parameter and local skin friction coefficient are two important fundamental parameters to be considered in this area  $Cf_r = \frac{\tau_w}{\rho(u_w)^2}$  and

$Nu_r = \frac{rq_w(r)}{k_f [T_f - T_s]}$  correspondingly. In non-dimensional system these quantities can be written as

$$C_f Re^{\frac{1}{2}} = (1 + A_1 \phi + A_2 \phi^2) f''(0), Nu Re^{-\frac{1}{2}} = -\frac{k_{nf}}{k_f} \theta'(0).$$

### Numerical Explanation.

Given the highly nonlinear forms of the equations (8) and (9), they are converted to an initial value problem together with the BCs (10) & (11) as used in MATLAB's BVP4C solver. Substituting this expression to equation (8) transforms it into a first-order differential equation although equation (9) is a second-order differential equation, it can be simply transformed into first-order differential by applying this substitution.

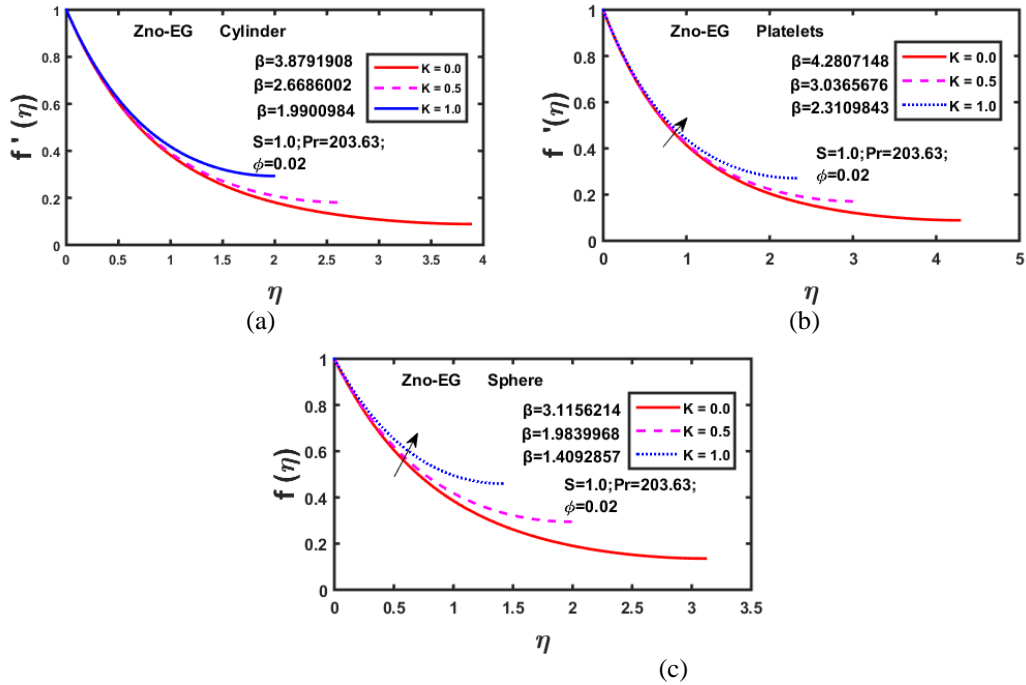
$$\begin{aligned} f' &= R'_{(1)} i = iR_{(2)}, f'' = R'_{(2)} = iR_{(3)} \\ f''' &= R'_{(3)} = \frac{1}{\epsilon_1} (S(R_{(2)} + tR_{(3)}) - 2R_{(1)}R_{(3)}) + (R_{(2)})^2, & \theta &= \\ &R_{(4)}, \theta' = R'_{(4)} = R_{(5)}, \\ \theta'' &= R'_{(5)} = \frac{Pr}{\epsilon_2} \left( \left( \frac{S}{2} \right) (3R_{(4)} + tR_{(5)} + 2R_{(4)}R_{(2)} - 2R_{(1)}R_{(5)}) \right) \end{aligned}$$

The corresponding BC's are:

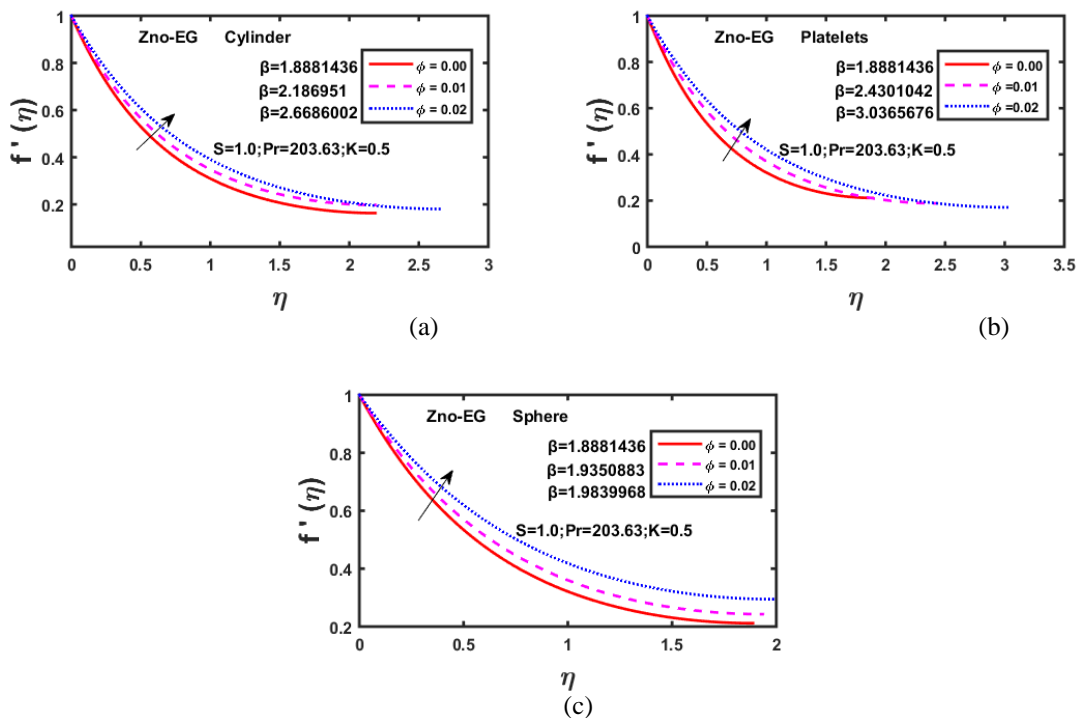
$$\begin{aligned} R_{(1)}(0) &= 0, R_{(2)}(0) = 1 \\ R_{(3)}(\beta) &= 0, R_{(4)}(0) = 1, R_{(5)}(\beta) = 0, R_{(1)}(\beta) = \frac{S\beta}{4} \end{aligned}$$

**II. Result and Discussion:-**

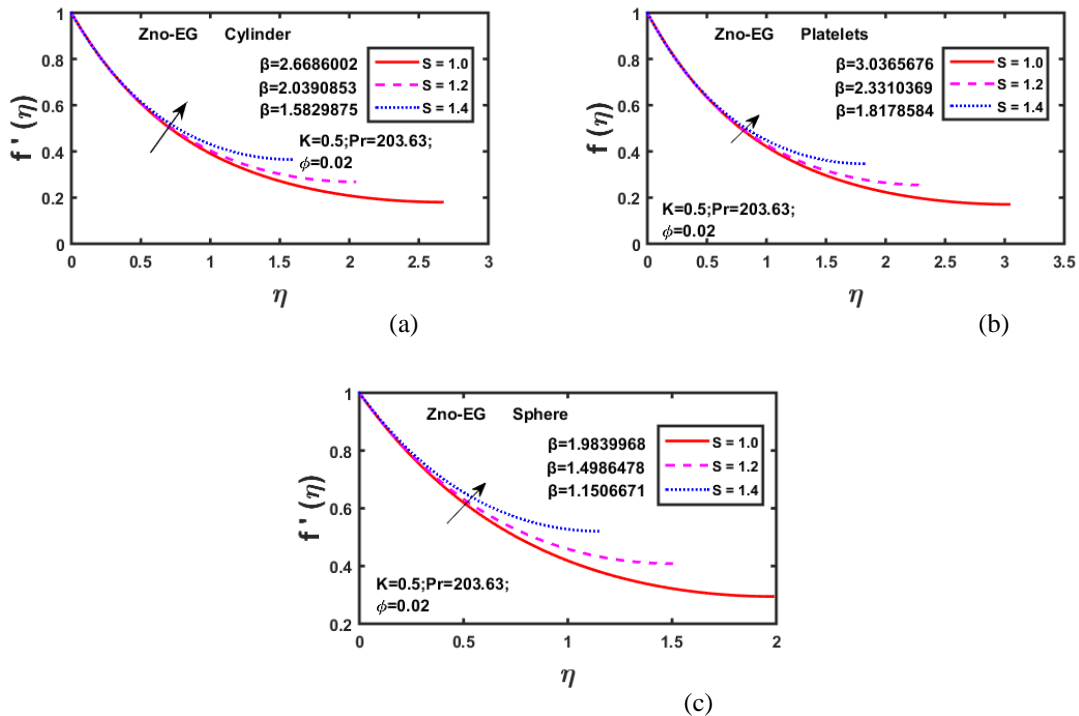
This article provides a method for solving the thin-film problem. The following explanation explains how numbers and film thickness ( $\beta$ ) affect heat transfer coefficient, skin friction, velocity, temperature. Figs 2(a-c) display the effect of the thermal conductivity number ( $K$ ) on the velocity distribution. Lorentz forces have a retarding impact, which causes the velocity field and  $\beta$  to decrease as  $K$  increases. Decelerating forces upsurge frictional resistance, which finally against liquid flow. Figs 3(a-c) show the effect of volumetric friction number ( $\phi$ ) on the film thickness and velocity profile. As  $\phi$  grows, velocity and film thickness increase. Figs 4(a-c) demonstrate the effect of the unsteadiness number ( $S$ ) on temperature profile. The parameter  $S$  rises as the temperature declines. There is no question that the unsteadiness number improves heat transmission.



**Figs. 2 (a-c):** Impact of  $f'$  over  $k$ .

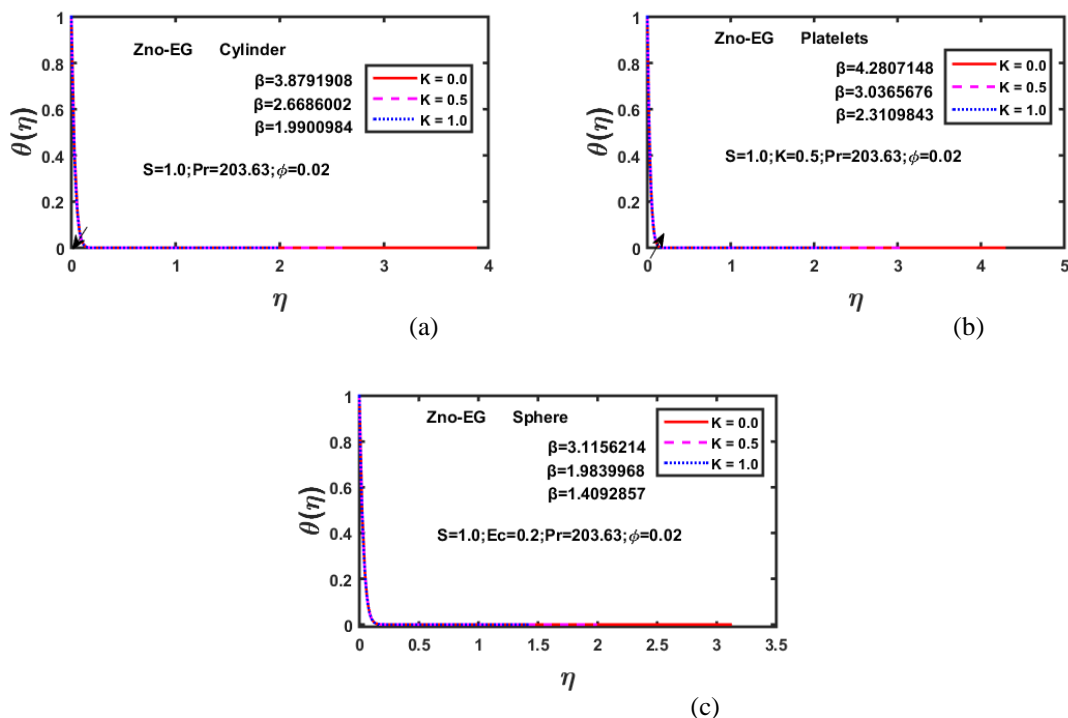


**Figs. 3 (a-c):** Impact of  $f'$  over  $\phi$ .

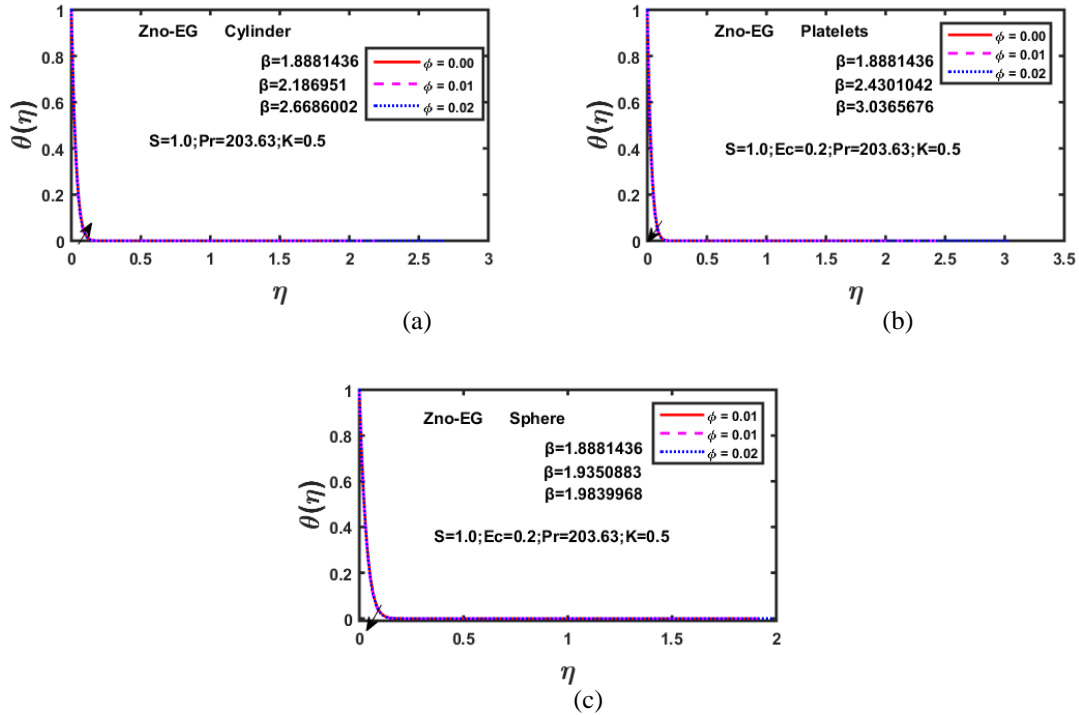


Figs. 4 (a-c): Impact of  $f'$  over  $S$ .

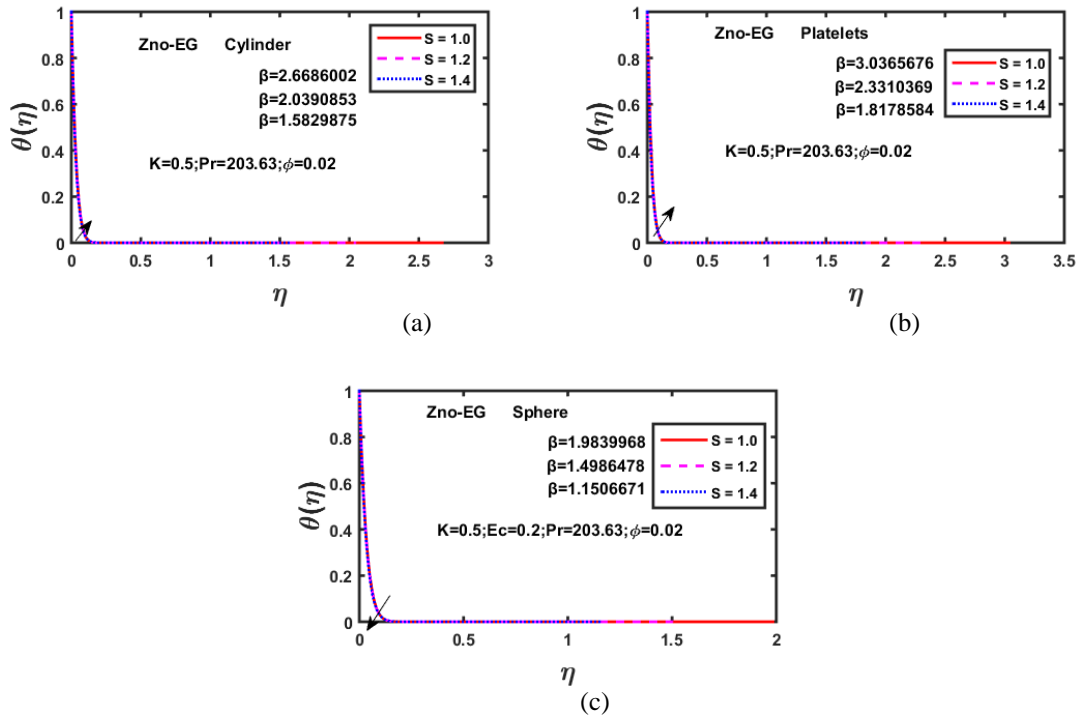
Figs 4(a-c) show that growing the thermal conductivity number  $K$  leads to a reduction in film thickness  $\beta$ . Because it transmits small heat from the sheet to the nanoliquids in the boundary layer segment, the extending sheet velocity decreases as the  $K$  upsurges. Figure 5(a-c) illustrates how film thickness and temperature change with growing  $\phi$ . As  $\phi$  grows, temperature falls. Figures 6(a-c) show that growing the unsteadiness number  $S$  leads to a drop in temperature and film thickness  $\beta$ . Because it transmits few heat from the sheet to the nanofluids in the boundary film segment, stretched sheet velocity decreases as unsteadiness parameter rises. Figures 7(a-c) show that when the value of  $Ec$  increases, so does the temperature declines. The frictional heating method causes the nanoliquid particles to maintain energy, allowing them to increase their  $Ec$  values.



Figs. 5 (a-c): Impact of  $\theta$  over  $K$ .



Figs. 6 (a-c): Impact of  $\theta$  over  $\phi$ .



Figs. 7 (a-c): Impact of  $\theta$  over  $S$ .

### Effect of Nusselt Number and Skin friction Coefficient

Since suspended nanoparticles have a longer residence time in the base fluid and a higher surface area-to-volume ratio compared to base fluids, the base fluid exhibits higher skin friction coefficients than nanofluids. Due to their lower skin friction, nanofluids can be utilized as lubricants. These properties enhance the flow characteristics of nanofluids. The Nusselt number represents the ratio of heat transfer by convection to conduction across a specific layer of fluid. A higher Nusselt number indicates more efficient convective heat transfer. Tables 1 and 2 show that the magnitude of the skin friction coefficient increases with  $S$  and  $\phi$  while it decreases with  $K$ .

The Nusselt number increases with higher values of  $Ec, \phi$ , and  $S$ , and decreases with higher values of  $K$ , as shown in the tables.

**Table1:** Skin-friction coefficient numerical values for multi-shape nanoparticles.

K	$\phi$	S	$C_f Re^{\frac{1}{2}}$		
			Cylinder	Platelets	Sphere
0.5	0.02	1.0	-1.6932582	-1.8707648	-1.6554049
0.0	-	-	-1.7054254	-1.8819491	-1.7011407
1.0	-	-	-1.6560094	-1.8376736	-1.5509734
-	0.00	-	-1.3327856	-1.3327856	-1.3327856
-	0.01	-	-1.4713264	-1.5927747	-1.4596025
-	0.02	1.2	-1.7246179	-1.9085519	-1.6514713
-	-	1.4	-1.7376967	-1.9285827	-1.6158368

**Table2:** Nusselt parameter numerical values for multi-shape nanoparticles.

K	$\phi$	S	$Nu Re^{-\frac{1}{2}}$		
			Cylinder	Platelets	Sphere
0.5	0.02	1.0	30.453241	30.694771	29.89746
0.0	-	-	30.451597	30.694584	33.314862
1.0	-	-	30.46132	30.696479	32.815798
-	0.00	-	30.462704	30.704571	32.048678
-	0.01	-	29.389325	29.388832	32.618329
-	0.02	1.2	31.30386	31.545586	30.733186
-	-	1.4	32.135386	32.384611	31.554494

### III. Conclusion

The study investigates the impact of a heat transfer on the unsteady thin film flow of a nanofluid over a radially stretched sheet, considering slip and convective conditions. The partial differential equations (PDEs) are reduced to a system of ordinary differential equations (ODEs), which are solved numerically using the bvp4c function. Various scenarios based on the radially stretching sheet are analyzed to determine how different physical parameters affect velocity and temperature.

- The velocity profile decreases with increasing values of (K), but increases with higher values of (S) and  $\phi$ .
- The findings indicate that nanoparticles with a platelet shape result in the greatest film thickness  $\beta$ , while spherical nanoparticles yield the smallest.
- The study reveals that platelet-shaped nanoparticles exhibit the highest skin friction and heat transfer rate coefficients, whereas cylindrical and spherical shapes have the lowest.
- For nanoparticles, cylinder and platelet shapes achieve the highest Nusselt number, while spherical shapes have the lowest. Temperature increases with higher values of K and S, but decreases with increasing values of  $\phi$ ,

### REFERENCES

[1]. B. Mehta, D. Subhedar, H. Panchal, and Z. Said, "Synthesis, stability, thermophysical properties and heat transfer applications of nanofluid – A review," J. Mol. Liq., vol. 364, p. 120034, 2022, doi: 10.1016/j.molliq.2022.120034.

[2]. A. G. N. Sofiah, M. Samykano, A. K. Pandey, K. Kadirgama, K. Sharma, and R. Saidur, "Immense impact from small particles: Review on stability and thermophysical properties of nanofluids," Sustain. Ener. Tech. Assess., vol. 48. 2021. doi: 10.1016/j.seta.2021.101635.

[3]. O. Mahian, E. Bellos, C. N. Markides, R. A. Taylor, A. Alagumalai, L. Yang, C. Qin, B. J. Lee, G. Ahmadi, M. R. Safaei et al., "Recent advances in using nanofluids in renewable energy systems and the environmental implications of their uptake," Nano Energy,

vol. 86, p. 106069, 2021.

- [4]. M. H. Esfe, M. Bahiraei, and A. Mir, "Application of conventional and hybrid nanofluids in different machining processes: A critical review," *Advances in Colloid and Interface science*, vol. 282, p. 102199, 2020.
- [5]. M. Amani, P. Amani, C. Jumholkul, O. Mahian, and S. Wongwises, "Hydrothermal optimization of  $\text{SiO}_2/\text{water}$  nanofluids based on attitudes in decision making," *International Communications in Heat and Mass Transfer*, vol. 90, pp. 67–72, 2018.
- [6]. A. Nikolov, P. Wu, and D. Wasan, "Structure and stability of nanofluid films wetting solids: An overview," *Advances in Colloid and Interface Science*, vol. 264, pp. 1–10, 2019.
- [7]. M. Amani, P. Amani, O. Mahian, and P. Estell'e, "Multi-objective optimization of thermophysical properties of eco-friendly organic nanofluids," *Journal of Cleaner Production*, vol. 166, pp. 350–359, 2017.
- [8]. G. Lu, X.-D. Wang, and Y.-Y. Duan, "A critical review of dynamic wetting by complex fluids: from newtonian fluids to non-newtonian fluids and nanofluids," *Advances in colloid and interface science*, vol. 236, pp. 43–62, 2016.
- [9]. S. Kumar, S. K. Prasad, and J. Banerjee, "Analysis of flow and thermal field in nanofluid using a single phase thermal dispersion model," *Applied Mathematical Modelling*, vol. 34, no. 3, pp. 573–592, 2010.
- [10]. S. U. Choi and J. A. Eastman, "Enhancing thermal conductivity of fluids with nanoparticles," Argonne National Lab. (ANL), Argonne, IL (United States), Tech. Rep., 1995.
- [11]. H. Masuda, A. Ebata, and K. Teramae, "Alteration of thermal conductivity and viscosity of liquid by Dispersing ultra-fine particles. Dispersion of  $\text{Al}_2\text{O}_3$ ,  $\text{SiO}_2$  and  $\text{TiO}_2$  ultra-fine particles," 1993.
- [12]. A. Majidian, M. Fakour, and A. Vahabzadeh, "Analytical investigation of the laminar viscous flow in a semi-porous channel in the presence of a uniform magnetic field," *International Journal of Partial Differential Equations and Applications*, vol. 2, no. 4, pp. 79–85, 2014.
- [13]. A. Vahabzadeh, M. Fakour, D. Ganji, and I. Rahimpetroudi, "Analytical accuracy of the one di-mensional heat transfer in geometry with logarithmic various surfaces," *Central European Journal of Engineering*, vol. 4, pp. 341–351, 2014.
- [14]. M. Fakour, A. Vahabzadeh, and D. Ganji, "Scrutiny of mixed convection flow of a nanofluid in a vertical channel," *Case Studies in Thermal Engineering*, vol. 4, pp. 15–23, 2014.
- [15]. D. D. Ganji, M. Fakour, A. Vahabzadeh, and S. H. H. KACHAPI, "Accuracy of vim, hpm and adm in solving nonlinear equations for the steady three-dimensional flow of a walter's b fluid in vertical channel," *Walailak Journal of Science and Technology (WJST)*, vol. 11, no. 7, pp. 593–609, 2014.
- [16]. M. Sheikholeslami, M. Hatami, and D. Ganji, "Nanofluid flow and heat transfer in a rotating system in the presence of a magnetic field," *Journal of Molecular liquids*, vol. 190, pp. 112–120, 2014.5
- [17]. M. Hatami and D. Ganji, "Thermal performance of circular convective–radiative porous fins with different section shapes and materials," *Energy Conversion and Management*, vol. 76, pp. 185–193, 2013.
- [18]. A. Vahabzadeh, D. Ganji, and M. Abbasi, "Analytical investigation of porous pin fins with variable section in fully-wet conditions," *Case Studies in Thermal Engineering*, vol. 5, pp. 1–12, 2015.
- [19]. M. Hatami, M. Sheikholeslami, and D. Ganji, "Retracted: Laminar flow and heat transfer of nanofluid between contracting and rotating disks by least square method," 2014.
- [20]. M. Hatami and D. Ganji, "Heat transfer and nanofluid flow in suction and blowing process between parallel disks in presence of variable magnetic field," *Journal of Molecular Liquids*, vol. 190, pp. 159–168, 2014.